Chapter 4 Diode-pumped nonlinear mirror mode-locking $Nd:GdVO_4$ Laser

4-1 Experimental setup

In nonlinear mirror experiment, the setup is almost the same as in SESAM, except for last two optical elements in our laser cavity, i.e.,

1. SESAM exchange for the R = 200 mm curvature mirror with both 1064 nm and 532 nm high reflectivity.
2. an output coupler (OC) exchange for the reflectivity of 80% at 1064 nm and high reflectivity at 532 nm dichroic flat mirror, a 10 mm long type-II KTP crystal with antireflection coated at both faces for wavelength 1064 and 532 nm was placed very close to the dichroic OC mirror for SH generation as Fig. 4.1.

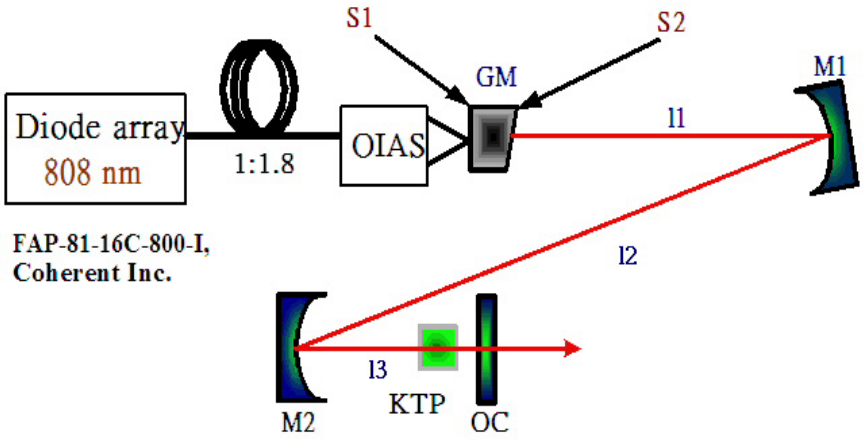

Fig. 4.1 Experiment configuration of nonlinear mirror mode locking.

4-2 Experimental results

4-2-1 Pico-second solid-state laser by nonlinear mirror mode-locking

First, we present our passive mode-locking with NLM results. In Fig. 4.2, we can see many states with different pump versus output power. And the slope efficiency is

about 25% for CW lasing operation. Vary large regime is for CW mode-locking output around 2 to 10 W. Fig. 4.3 is the result of CW mode-locking on oscilloscope, pulse train is regular with 8 ns spacing.

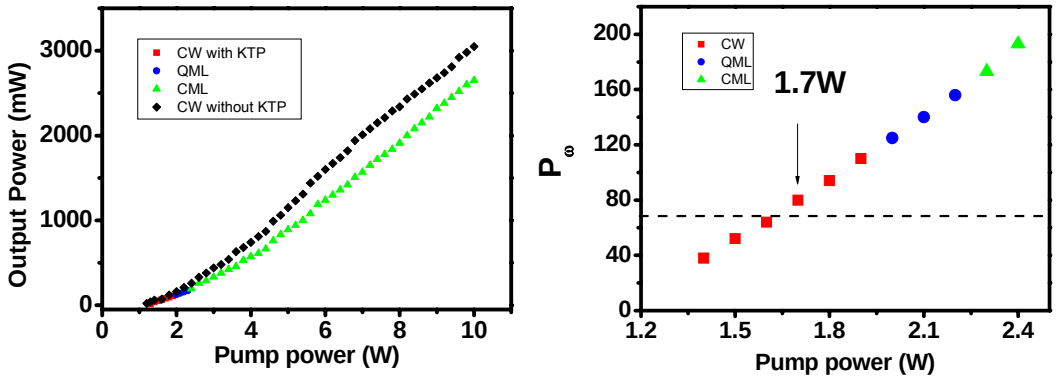

Fig. 4.2 Output and pump power with different operation states such as : CW, and QML, CML.

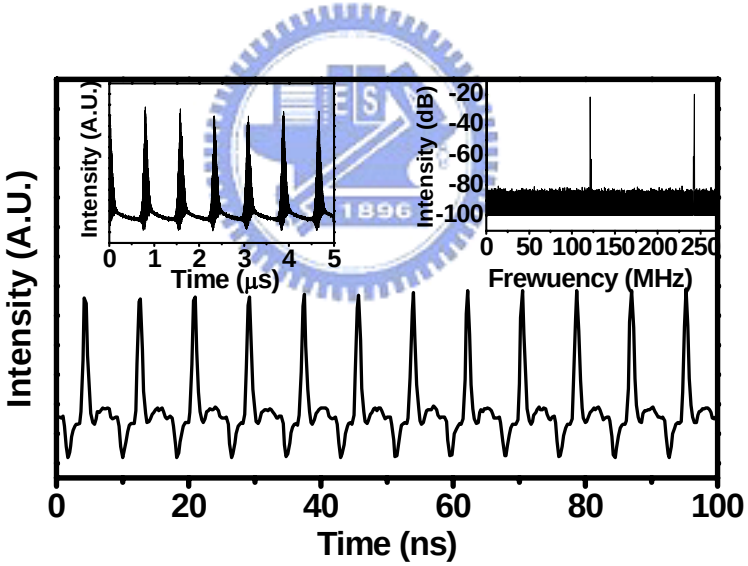

Fig. 4.3 Oscilloscope and RF spectrum results of mode locking with nonlinear mirror.

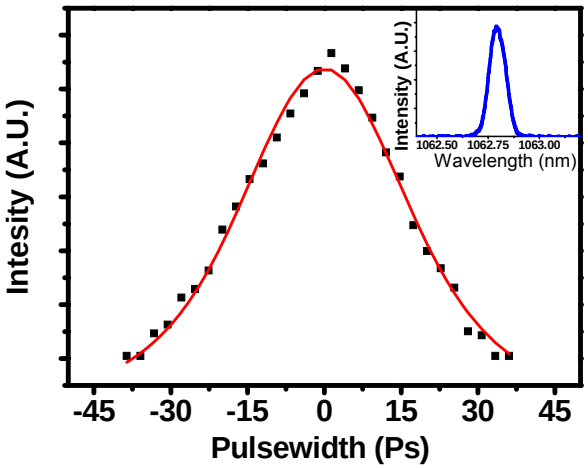

Fig. 4.4 Autocorrelation of passive mode locking with 10mm KTP nonlinear mirror and spectrum inserted.

Both time trace and RF spectrum of the Q-switching mode-locking were shown in the insets of Fig. 4.3. We also measured the pulse-width using the homemade autocorrelator to be ~ 37 ps and the bandwidth to be 0.4 nm as the inset in Fig. 4.4

4-2-2 Harmonic mode locking

As we knew, two-pulse generation of Kerr-lens mode-locked Ti:sapphire laser has been reported [1-3]. The most detailed experimental investigation on fs-pulse splitting and multiple pulse operation had been performed in the works [4-5]. But, to our knowledge there has no report on pulse splitting in pico-second passive NLM-MLlaser. In this thesis, we observed the pulse splitting in two ways by moving the nonlinear crystal in the cavity and increasing the pumping power.

(a) Varying the distance between the KTP and dichroic mirror

When KTP is moved toward the dichoric mirror, we observed the pulse splitting and harmonic mode locking recorded on the oscilloscope and RF spectrum analyzer. Besides,

we also found that the average output power is increasing with moving the KTP. Shown in Fig. 4.5 are the pulse trains and corresponding rf spectra for the normal mode locking (NML), the second harmonic mode locking (SHML), the third harmonic mode locking (THML) and the fourth harmonic mode locking (FHML), respectively. The NML is displayed on Fig. 4.5(a) and (b) whose period of pulse train is equal to cavity round trip time and the fundamental frequencies on the rf spectrum are the multiple of longitudinal mode spacing. Time trace of the SHML in Fig. 4.5(c) reveals the numbers of pulses are twice of that in Fig. 4.5(a). Furthermore, the spectral peaks at the first and the third harmonics of longitudinal mode spacing are suppressed below the noise level in Fig. 4.5(d) demonstrating the pulse trains with highly periodic. Similarly, THML and FHML are shown in Fig. 4.5(e)-(h) with 1/3 and 1/4 times cavity round trip period of pulse spacing in time traces.

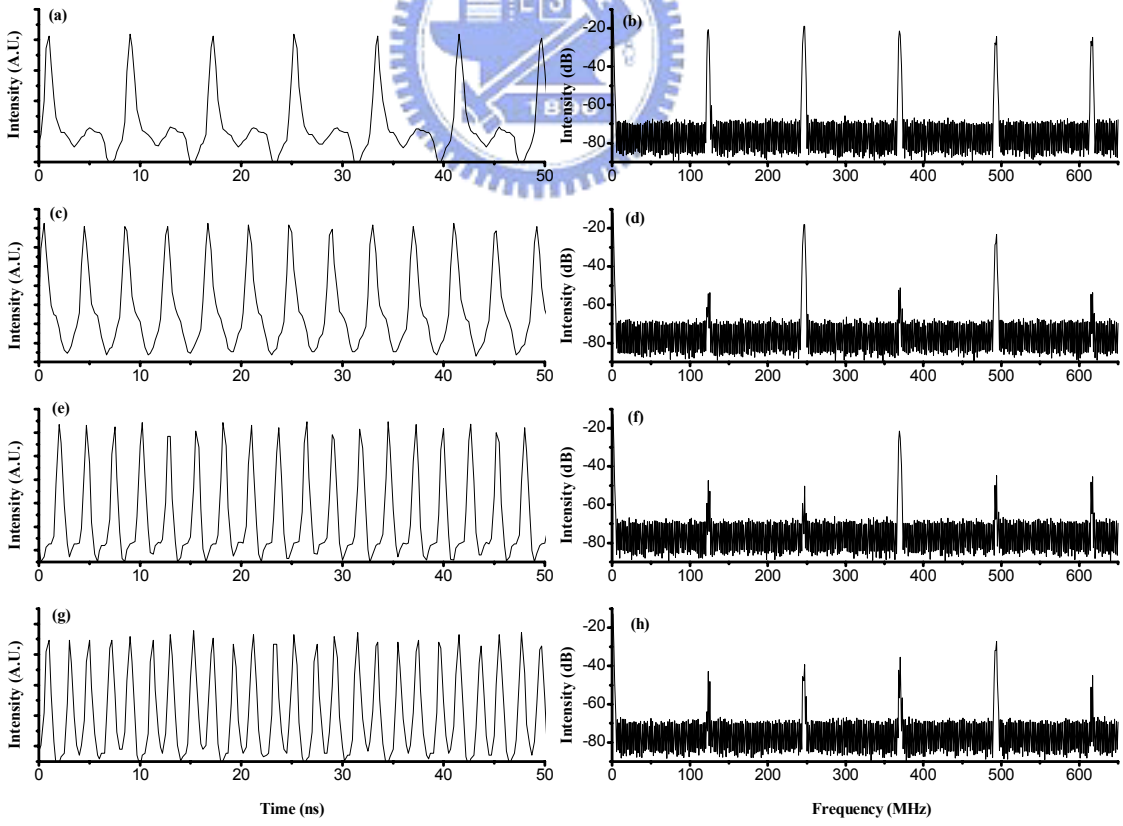

Fig. 4.5 Pulse trains and their corresponding rf spectra for the NLM [(a) and(b)], SHML [(c) and(d)], THML [(e) and(f)], and FHML [(g) and(h)], respectively.

(b) Increasing the pumping power

Varying the distance between the KTP and dichroic mirror is not an easy way to achieve pulse-splitting phenomena. So we want to make it easier to produce the pulse splitting by increasing pumping power. The reason for changing this experiment parameter is that we think varying the distance is equivalent to change the intensity on the KTP because of effectively changing the reflection modulation ΔR. In Fig. 4.6, the different multi-pulsing state versus pumping power is shown. We found the SHML starts at pumping power ~ 4W. The boundary of the stable mode locking with small signal gain versus unsaturated loss was proposed by Haus [6]. Thus, it inspires us whether we can find out the power dependence of gain and loss for explanation of harmonic mode locking (dealt in later section). More information can be found from Fig. 4.6 which shows increasing pumping power the state will transfer from CML to SHML or THML, FHML. In the SHML mode locking pumping regime, we can also see the CML by moving the KTP, and so as in the THML regime (SHML and CML can been seen) and in the FHML (THML and SHML can been seen). The phenomena give the powerful evidence for our motive.

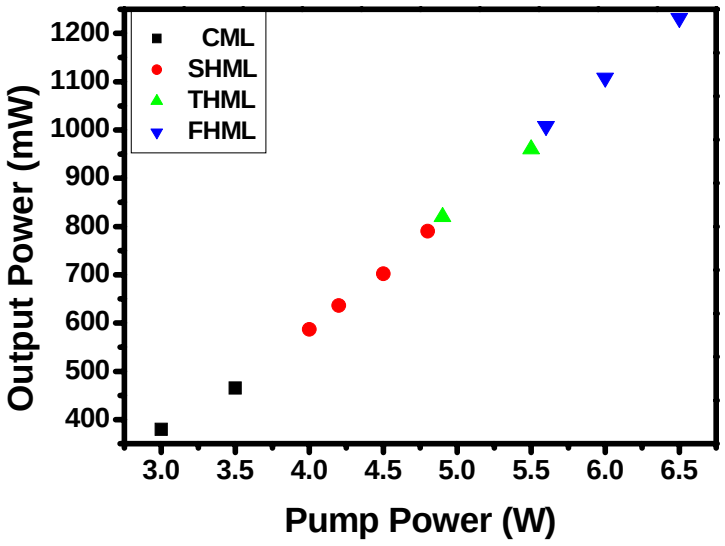

Fig. 4.6 Regime of CML, SHML, THML, FHML versus pumping power.

4-3 Discussion

The threshold power of 2.3 W for our stable CML is much lower than those of 9 W and 10 W for the nonlinear mirror mode-locking Nd:YVO_4 mode-locked laser with 15 mm LBO [6] and 3 mm KTP [7], respectively. It is also much lower than 13.6 W for the Nd:$GdVO_4$ mode-locked laser with SESAM [8]. We therefore estimate the threshold for the CML against the QML as the intra-cavity peak power P_ω exceeds the critical value (P_c) according to [9]:

$$\mathbf{P_\omega \geq P_c = (P_L P_A \Delta R_{max})^{1/2}}, \tag{4-3.1}$$

where P_L and P_A are the saturation power of the gain medium and the NLM "absorber", respectively, and ΔR_{max} is the maximum nonlinear modulation. Since the saturation intensity is related to the center frequency ω_o of the fundamental wave, the stimulated emission cross section $\sigma_L = 7.6 \times 10^{-19}$ (cm^2) and the fluorescence life time $\tau_f = 90\ \mu s$, we estimated the saturation power of the gain medium $P_L = I_s(\pi W_g^2)$ to be 3.8 W according to $\mathbf{I_{sat} = \frac{\hbar \omega_o}{\sigma_L T_L}}$ with $\hbar$ being the Planck constant. And the saturation power P_A of the NLM is defined as the ratio of the linear loss Q_c and the first order nonlinear loss modulation M introduced by NLM absorber [6] which satisfies

$$M = -(dL/dP_\omega)_{P_\omega=0} = -(dL_{nl}/dP_\omega)_{P_\omega=0} = -(\rho/P_\omega)R_\omega[R_\omega + 1 + 2\cos(\Delta kl - \Delta\phi)], \tag{4-3.2}$$

where $L = Q_c + L_{nl}$ is the round trip total loss and L_{nl} is the nonlinear loss, $\Delta\phi = \phi_{SH} - \phi_{FW}$ is the phase mismatch due to the dispersion of the air, and $\Delta k = k_{SH} - 2k_{FW}$ is the wave vector mismatch between the FW and the SH in NLC. For low conversion efficiency, the coefficient of the conversion efficiency ρ from the FW to the SH can be presented as [10]

$$\mathbf{\rho(P_\omega) = \frac{P_{2\omega}}{P_\omega} = l^2(2\eta^3\omega^2 d^2_{eff})(\frac{P_\omega}{A})\frac{\sin^2(\Delta kl/2)}{(\Delta kl/2)^2}}, \tag{4-3.3}$$

where $P_{2\omega}$ is the intra-cavity peak power of the second harmonic wave, A is the area of fundamental beam at the KTP, l is the length of the KTP, η is the plane-wave impedance,

and d_{eff} = 3.18 (pm/v) is the effective second order nonlinear coefficient. In considering the strong modulation with the situation $\Delta k = 0$ and $\Delta\phi = \pi$, the maximum nonlinear loss is estimated with $M_{max} = (\rho/P_\omega)R_\omega(1- R_\omega)$. Therefore, the saturation power $P_A = Q_c/M_{max}$ = 6.9 kW for 10 mm KTP, and $\Delta R_{max} = 1\text{-}R_\omega$ = 20%, if the nonsaturable loss is nearly zero at high P_ω. Thus, the critical peak power (P_c) of CML for nonlinear mirror is estimated around 72 W that can be reached as the pumping power is around 1.8 W as shown on the right hand side of Fig. 4-2. This value is slightly lower than our experimental result of 2.3 W for the stable CML that may be due to overestimating P_ω at the lower pumping with the broader pulse-width.

In the following, we try to find out the boundary against stability mode locking the same as multi-pulsing regime proposed in the previous work [11] to fit our experiment. In our case (passive mode-locking in pico-second regime), our optical component such as Nd-doped laser crystal, KTP and mirror is assumed dispersionless. So we use the Ginzburg-Landau equation which can be derived from Eq. (2-3.11) to describe this system:

$$[1 + q_0 - g(1 + \frac{1}{\omega_L{}^2}\frac{d^2}{dt^2})]\upsilon - q_0\frac{|\upsilon|^2}{P_A} = 0. \qquad (4\text{-}3.4)$$

Here q_0 is unsaturated loss coefficient, ω_L is gain medium line width, P_A is absorber's saturation power, υ is slowly time varying envelope amplitude, and g is the normalized saturated gain coefficient that can be expressed as

$$g = \frac{g_0}{1 + \frac{P}{P_L}}, \qquad (4\text{-}3.5)$$

where g_0 is the normalized small-signal gain coefficient, which is normalized by the linear loss Q_c as

$$g_0 = \frac{1}{2}\frac{g_0'}{Q_c}. \qquad (4\text{-}3.6)$$

Here g_0', the small-signal gain coefficient, has the form

$$g_0' = 2l\sigma_{21}\tau_f\eta_Q\eta_S\eta_B\frac{P_{ab}}{h\upsilon_L V}, \tag{4-3.7}$$

where l, σ_{21}, τ_f are the length, stimulated emission cross section, fluorescence time of gain medium, η_Q is the external quantum efficiency, η_S is the Stoke's efficiency, η_B is the beam overlap efficiency, P_{ab} is the pumping power, υ_L is the lasing frequency, and V is the lasing beam volume in gain medium.

The term in Eq (4-3.4) contained q_0 is the absorber loss and the differential term is the dispersion of laser medium with line-width ω_L. We assume the solution is pulse-like hyperbolic secant

$$\upsilon(t) = \upsilon_0 \operatorname{sech}(t/\tau_p), \tag{4-3.8}$$

where τ_p is the pulse width. There are two steady-state solutions

$$q_0\frac{\upsilon_0^2}{P_A} = \frac{2g}{\omega_L^2\tau_P^2}, \tag{4-3.9}$$

$$1 - q_0 - g = \frac{g}{\omega_L^2\tau_P^2}. \tag{4-3.10}$$

By introducing a control parameter K

$$K \equiv \frac{1}{4}(P_L/P_A)\omega_L\tau_P, \tag{4-3.11}$$

which is almost the same as the ratio of the saturation power of gain medium and absorber, we substitute Eq. (4-3.11) into (4-3.9) and get

$$qK\frac{P}{P_L} = \frac{g}{\omega_L\tau_P}; \tag{4-3.12}$$

and substitute Eq. (4-3.10) into (4-3.12) to obtain

$$\frac{qK}{1+q}\frac{P}{P_L} = (\omega_L\tau_P + \frac{1}{\omega_L\tau_P})^{-1}. \tag{4-3.13}$$

Therefore, (4-3.10) becomes

$$\frac{g_0}{1+q}(\omega_L\tau_P + \frac{1}{\omega_L\tau_P})^2 = \omega_L\tau_P(\omega_L\tau_P + \frac{1}{\omega_L\tau_P} + \frac{1+q}{qK}). \tag{4-3.14}$$

We plot the steady state solution of Eqs. (4-3.13) and (4-3.14) with parameter $g_0/1+q_0$ from

1.2 to 2 with 0.1 increment shown in Fig. 4.7 and Fig. 4.8 with $g_0/1+q_0$ from 1.1 to 2.5 with 0.4 increment.

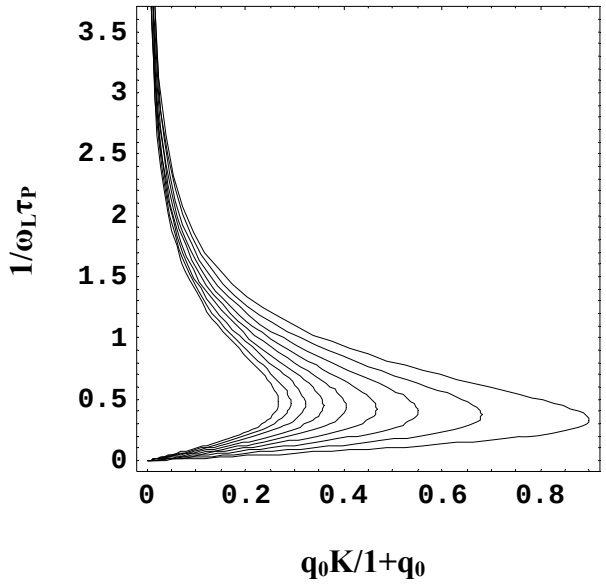

Fig. 4.7 The inverse pulse width ($1/\omega_L\tau_P$) versus $q_0K/1+q_0$.

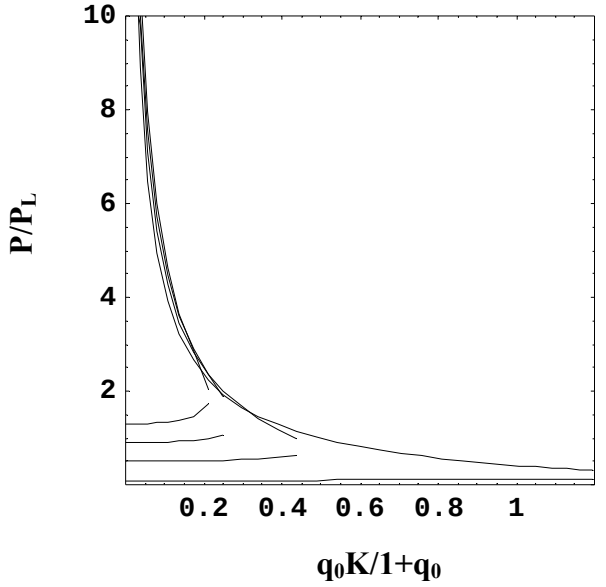

Fig. 4.8 Power (proportional to pulse energy) versus $q_0K/1+q_0$.

From Figs. 4.7 and 4.8, we can see two branches (two-valued functions), however, there should have only one correct solution in a laser system. Fig. 4.7 gives us the important clues because of the limiting $1/\omega_L\tau_P < 1$, in the other word, τ_P, the pulse-width,

should always be larger than the inverse of line width ω_L. As a result, we can quickly distinguish the lower part in both Figs. 4.7 and 4.8 are the correct solutions. In Fig. 4.7, the locus of apices is the boundary for each condition, and therefore we can obtain the boundary that determines q_0 as the following formula:

$$\frac{q_0 K}{1+q_0} = (1 - \frac{3}{(\omega_L \tau_P)^2})[\frac{2}{\omega_L \tau_P}(1 + \frac{1}{\omega_L{}^2 \tau_P{}^2})]^{-1}. \qquad (4\text{-}3.15)$$

We plot the boundary determined by Eqs. (4-3.14) and (4-3-15) in terms of g_0 versus q_0 as Fig. 4-9. Ten black spots are the experiment data from bottom to top representing the pumping power changing from 1W to 10W using Eqs. (4-3.6) and (4-3.7). The red star is the threshold of acquiring CML from Fig. 4-2. We found from Fig. 4-9 that the theoretical boundary of CML and HML or threshold of multipulsing is at the pump power of 4.5 W, which agrees quite well with our previous experimental result of 4 W from Fig. 4-6.

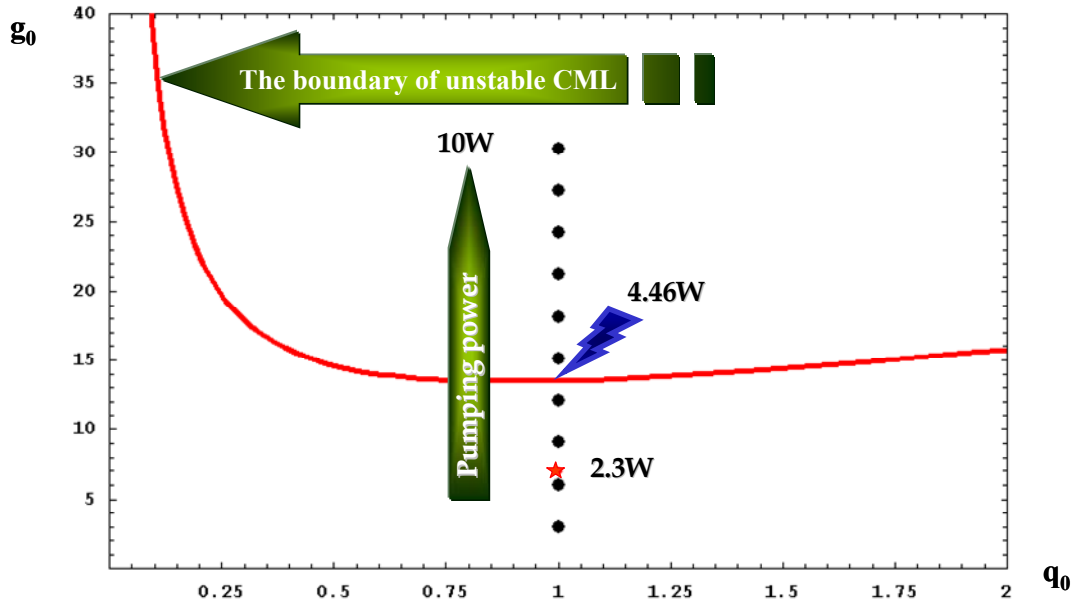

Fig. 4-9 Boundary of CML and HML. The experiment results in black spots with increasing pumping power. Red star represents the experimental CML threshold.

Using this method, we can estimate the criterion of HML under many different laser conditions and it's the nice way to predict the condition of multi-pulsing for preventing this

instability. It also gives the power dependence of the small signal g_0, and therefore one can also observe the state change with varying pumping power.

The motivation for this experiment is originally to produce high peak-power laser pulses, but here we observed mutipulsing phenomena and obtained the threshold for NLM-ML instead. We will discuss how to achieve high peak-power laser pulses in our NLM-ML experiment along with previous SESAM case in the next chapter.

References

[1] J.-C. Diels, and W. Rudolph, ”Ultrashort Laser Pulse Phenomena,“ Academic Press, San Diego, (1996).

[2] D. R. Dykaar, S. B. Darack, and W. H. Knox, ”Cross-locking dynamics in a two-color mode-locked Ti:sapphire laser, ” Opt. Lett. 19, 1058 (1994).

[3] A. Leitenstorfer, C. Furst, and A. Laubereau, ”Widely tunable two-color mode-locked Ti:sapphire laser with pulse jitter of less than 2 fs,” Opt. Lett. 20, 916 (1995).

[4] M. Lai, J. Nicholson, and W. Rudolph, ”Multiple pulse operation of a femtosecond Ti:sapphire laser, ” Opt. Commun. 142, 45 (1997).

[5] C. Wang, W. Zhang, K. F. Lee, and K. M. Yoo, ”Pulse splitting in a self mode- locked Ti:sapphire laser, ” Opt. Commun. 137, 89 (1997).

[6] P. K. Datta, S. Mukhopadhyay, and A. Agnesi, “ Stability regime study of a nonlinear mirror mode-locked laser,” Opt. Commun. 230, 411 (2004).

[7] Y. F. Chen, S. W. Tsai, and S. C.Wang, “High-power diode-pumped nonlinear mirror mode-locked Nd:YVO_4 laser with periodically-poled KTP,” Appl. Phys. B-Laser and Optics, 72, 395 (2001).

[8] S. Zhang, E. Wu, H. Pan and H. Zeng, ”Passive mode locking in a diode-pumped Nd:GdVO4 laser with a semiconductor saturable absorber mirror,” IEEE J. Quantum. Electron. 40, 505 (2004).

[9] C. Ho¨nninger, R. Paschotta, F. Morier-Genoud, M. Moser, and U. Keller, “Q-switching stability limits of continuous-wave passive mode locking,” J. Opt. Soc. Am. B, 16, pp. 46 (1999).

[10] W. Koechner, Soild-state laser engineering, E. D. A. L. Schawlow, A. E. Siegman, T. Tamir, fifth ed., Springer, Berlin, Heidelberg (1999).

[11] Hermann A. Haus, “Parameter ranges for CW passive mode locking,” IEEE J. Quantum Electron. 12, 169 (1976).